

Screened Coulomb interactions between finite-sized macroions of various shapes

Jeffrey C. Everts^{1,*}

¹*Faculty of Mathematics and Physics, University of Ljubljana, Jadranska 19, 1000 Ljubljana, Slovenia*

(Dated: May 29, 2022)

A semi-analytical approach is developed to calculate the effective pair potential of rigid arbitrarily-shaped macroions with a non-vanishing particle volume, valid within linear screening theory and the mean-field approximation. The essential ingredient for this framework is a mapping of the particle to a singular charge distribution with adjustable effective charge and shape parameters determined by the particle surface electrostatic potential. For charged spheres this method reproduces the well-known Derjaguin-Landau-Verwey-Overbeek (DLVO) potential. Further exemplary benchmarks of the method for more complicated cases, like tori, tri-axial ellipsoids, and additive torus-sphere mixtures, leads to accurate closed-form integral expressions for *all* particle separations and orientations, not yet known in the literature. The findings are relevant for determining the phase behaviour of macroions with experiments and simulations for various particle shapes.

Screened Coulomb interactions of electronic or ionic nature are ubiquitous in quantum-mechanical and classical systems, such as strongly correlated electron matter [1, 2], chemical bonds [3, 4], superconductors [5], proteins [6], liquid crystals [7–9], DNA [10–12], graphene [13], lipid membranes [14, 15], supercapacitors [16, 17], microfluidics [18], and dusty plasmas [19, 20]. A general understanding of electrostatic screening in various geometrical settings is needed, considering that many of these systems have a complex geometry. In particular, classical charge-screened particles of various shapes and surface functionalities can be experimentally synthesised and characterised today in great detail [21, 22], however, theoretical understanding of effective particle interactions is lagging behind as it is difficult to account for finite particle volume and non-spherical particle shape. This letter is aimed at bridging the gap between the available experimental and theoretical toolkit.

In order to express the system in solely the degrees of freedom of interest — such as the positions and orientations of specific particles — it is useful to integrate out the “fast” charge degrees of freedom, which leads to an effective description in terms of electrostatic screening. In free-electron like metals this procedure leads to Friedel oscillations, electron density modulations near a solid-fluid interface and around impurities [23–25], which is a canonical example of an emergent phenomenon caused by screening. In classical systems [26] and sufficiently dilute quantum systems [27, 28], screening is often associated with the damped spatial decay of the electrostatic potential (and thus the effective pair potential), that for point particles and for low voltages compared to the thermal energy, has the Yukawa form, $\sim \exp(-\kappa r)/r$, with κ^{-1} the Debye screening length and r the radial distance, as opposed to the bare Coulomb case $\sim 1/r$. Of special interest are spherical charged particles, with radius a in the colloidal (sub-)micron regime, dispersed in

ion-containing liquids, because of their tunable charge and screening properties [29]. Integrating out the degrees of freedom of the smaller ions results in a Yukawa-type effective sphere-sphere potential with a prefactor that depends on the particle charge and, unlike for point particles, also the salt concentration via κa arising from the ion-impenetrable particle hard core [30, 31]. This so-called DLVO potential [32] is an essential theoretical tool for understanding the behaviour of charge-stabilised colloids [33], even for out-of-equilibrium suspensions [34].

For non-spherical shapes, the screened-electrostatic pair interaction is only analytically known in a few cases for all particle configurations, even within linear screening theory. However, some studies exist for disks [35–38], rods [39, 40], spheroids [41–45], or helices [46], where the potential is sometimes calculated only for infinitely long, thin, or ion-penetrable particles, restricted particle configurations or for orientation-averaged interactions [47]. The difficulty in finding analytical solutions lies in the finite ion-impenetrable particle volume which complicates matching the series expansion solution (if it is even available for the geometry under consideration) of the unscreened potential inside and the screened potential outside the particle via the boundary conditions. However, when the pair potential would be known, one does not need to numerically solve the 3D Poisson(-Boltzmann) equation for every single particle configuration at each simulation step, as in Refs. [48–50] for simulations of charged colloids. Instead, computationally less expensive simulations with effective pair potentials can be used, and by mapping to cell models, even charge regulation can be incorporated [51]. The lack of availability of accurate pair potentials might explain why fewer phase behaviour studies are known for complex-shaped charged particles [52–54] than for charge-neutral hard particles [55–60].

In this letter, I devise a framework to semi-analytically approximate effective interactions between (not necessarily equal) charged finite-size particles with not necessarily spherical shape. By mapping particles to singular charge distributions (i.e. expressed by δ functions), I find a

* jeffrey.everts@gmail.com

straightforward and accurate evaluation of the interaction free energy for *arbitrary* inter-particle separations and orientations. For spheres, this method reproduces DLVO theory, hence a similar level of approximation is expected such as weak double layer overlap [61]. After discussing spheres, I apply the framework to more complicated shapes, such as tori and ellipsoids.

To set up the theoretical framework, I consider an ion-impenetrable charged particle of arbitrary shape with dielectric constant ϵ_p , surface \mathcal{P} , and interior volume $\text{int}(\mathcal{P})$, immersed in a structureless solvent with dielectric constant ϵ_s and Bjerrum length $\ell_B = \beta e^2 / (4\pi\epsilon_0\epsilon_s)$, with e the proton charge, ϵ_0 the vacuum permittivity, and $\beta^{-1} = k_B T$, with k_B the Boltzmann constant and T temperature. By thermally averaging over the ions, an inhomogeneous electrostatic potential $\phi(\mathbf{r})/(\beta e)$ describes the electric double layer that is formed around the particle. I split the total electrostatic potential as a contribution inside the particle $\phi_{<}(\mathbf{r}) = \phi(\mathbf{r})|_{\mathbf{r} \in \text{int}(\mathcal{P})}$, and a contribution outside the particle $\phi_{>}(\mathbf{r}) = \phi(\mathbf{r})|_{\mathbf{r} \notin \text{int}(\mathcal{P})}$. For linear screening, $|\phi(\mathbf{r})| \ll 1$, and within the mean-field approximation, $\phi_{<}(\mathbf{r})$ and $\phi_{>}(\mathbf{r})$ are given by the Laplace and Debye-Hückel (DH) equation, respectively,

$$\nabla^2 \phi_{<}(\mathbf{r}) = 0, \quad \nabla^2 \phi_{>}(\mathbf{r}) = \kappa^2 \phi_{>}(\mathbf{r}), \quad (1)$$

with continuity $\phi_{<}(\mathbf{r}) = \phi_{>}(\mathbf{r})$ for $\mathbf{r} \in \mathcal{P}$, and constant-charge boundary condition on the particle surface with outward normal $\hat{\nu}$ and surface charge density $e\sigma$,

$$\hat{\nu} \cdot [\epsilon_p \nabla \phi_{<}(\mathbf{r}) - \epsilon_s \nabla \phi_{>}(\mathbf{r})] / \epsilon_s = 4\pi \ell_B \sigma, \quad \mathbf{r} \in \mathcal{P}. \quad (2)$$

The finite particle volume complicates matching $\phi_{>}(\mathbf{r})$ and $\phi_{<}(\mathbf{r})$ through the boundary conditions [42], although formal exact multiple-scattering expansions exist [62]. Sometimes Eq. (1) is not even separable in certain coordinate systems, which further complicates finding analytical solutions. For example, due to the non-separability of the Helmholtz equation (DH with imaginary κ) in toroidal coordinates, the complete solution can only be expressed in terms of lengthy toroidal wave functions [63]. However, some approximations for the double layer around a torus exist [64, 65].

The first central message of this letter is that an ion-impenetrable charged particle can be mapped to a singular charge distribution $q(\mathbf{r})$ *without* a particle hard core, described by the DH equation $(\nabla^2 - \kappa^2)\varphi(\mathbf{r}) = -4\pi\ell_B q(\mathbf{r})$, such that the outside potential is approximated to a very high accuracy by $\phi_{>}(\mathbf{r}) \approx \varphi(\mathbf{r})$. Consequently, $\varphi(\mathbf{r})$ can be expressed as the convolution of $q(\mathbf{r})$ with the DH Green's function,

$$\varphi(\mathbf{r}) = \ell_B \int d\mathbf{r}' q(\mathbf{r}') \frac{\exp(-\kappa|\mathbf{r} - \mathbf{r}'|)}{|\mathbf{r} - \mathbf{r}'|}. \quad (3)$$

Here, $q(\mathbf{r})$ can either be a point, line, or surface charge distribution and has to be parametrised with the same

symmetry of the particle. The salt-dependent shape and magnitude of $q(\mathbf{r})$ can be determined by matching, e.g. the numerically or analytically obtained surface potential. The benefit of this method is that the *same* $q(\mathbf{r})$ for a single particle, enters the approximate analytical expression for the charge-screened two-particle interaction, which is the second central message of this work.

As an example, a sphere of radius a and total charge $Z_s e = 4\pi a^2 \sigma e$ can be mapped to a point charge $q(\mathbf{r}) = Q_p \delta(\mathbf{r})$. Using Eq. (3) gives $\varphi(\mathbf{r}) = Q_p \ell_B \exp(-\kappa r) / r$, to be compared with the exact analytical solution [66]

$$\phi_{>}(\mathbf{r}) = \frac{Z_s \ell_B \exp(\kappa a) \exp(-\kappa r)}{1 + \kappa a} \frac{1}{r}. \quad (4)$$

Matching the potential on the particle surface, $\varphi(r=a) = \phi_{>}(r=a)$, I find $Q_p = Z_s \Upsilon_s$, with $\Upsilon_s = \exp(\kappa a) / (1 + \kappa a)$. Alternatively, Q_p can be computed: for the ion densities caused by the singular point charge within DH theory, $\rho_{\pm}(\mathbf{r}) = \rho_s \exp[\mp \varphi(\mathbf{r})] \approx \rho_s [1 \mp \varphi(\mathbf{r})]$, one can check that $Z_s = Q_p + \int_{r < a} d\mathbf{r} [\rho_+(\mathbf{r}) - \rho_-(\mathbf{r})]$ showing that an ion-impenetrable charged sphere produces the same electrostatic potential for $r > a$ as an ion-penetrable particle, consisting of a suitable point charge surrounded by a plasma of ions. This physical interpretation is possible because $\phi_{<}(\mathbf{r}) = Z_s \ell_B / [a(1 + \kappa a)]$ is constant and therefore does not contribute to Eq. (2).

To calculate two-particle interactions, I consider two charged bodies with their centre of masses located at position vectors $\mathbf{X}_{1,2}$ and particle orientations $\Omega_{1,2}$, represented by total singular charge distributions $q_T(\mathbf{r})$ and corresponding $\varphi_T(\mathbf{r})$ via Eq. (3). The effective Hamiltonian for this fixed configuration of particles is given in the DH approximation by

$$\beta \Phi_e(\mathbf{d}, \Omega_1, \Omega_2) = \frac{1}{2} \int d\mathbf{r} q_T(\mathbf{r}) \varphi_T(\mathbf{r}), \quad (5)$$

with center-to-center distance vector $\mathbf{d} = \mathbf{X}_1 - \mathbf{X}_2$. It is understood that the infinite self-energy terms are subtracted, and only fixed charges are included because the ion distributions are thermally averaged. For spherical particles, the DLVO potential results from Eq. (5),

$$\beta \Phi_e^{ss}(d) = Z_s^2 \ell_B \left[\frac{\exp(\kappa a)}{1 + \kappa a} \right]^2 \frac{\exp(-\kappa d)}{d}, \quad (6)$$

with $d = |\mathbf{d}|$. The same result follows from the linear superposition approximation (LSA) used on Eq. (4), $\phi_{2B}(\mathbf{r}) \approx \sum_i \phi_{>}(\mathbf{r} - \mathbf{X}_i)$, in force calculations with the stress tensor [66]. However, Eq. (5) is incompatible with the LSA: one would obtain a different result than Eq. (6) because the LSA does not account for ion-particle hard-core interactions [36]. In contrast, unique for the point-charge mapping is the compatibility with the free energy *and* the stress tensor route, because the particle hard core is effectively mapped out. Finally, I note that mapping spheres to ion-penetrable charged spherical

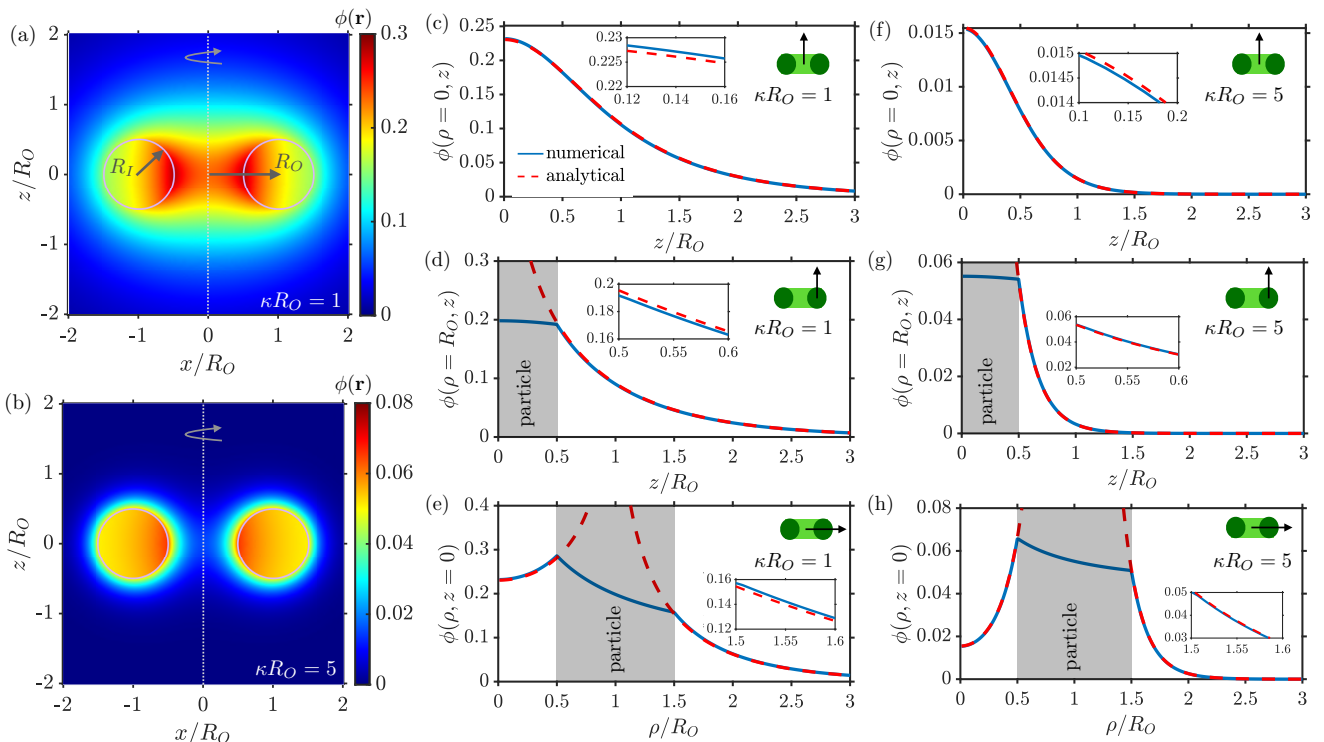


Figure 1. Electrostatic potential $\phi(\mathbf{r})/(\beta e)$ around a charged torus with charge $Z_t e = 50e$, $\epsilon_p/\epsilon_s = 0.2$, $\ell_B/R_O = 0.01$, and $R_I/R_O = 0.5$ for various κR_O . For $\kappa R_O = 1$ ($\kappa R_O = 5$), I found $\Upsilon_t = 1.22$ ($\Upsilon_t = 5.409$) and $R/R_O = 0.9863$ ($R/R_O = 1.027$). (a) Numerical results for thick and (b) thin double layers. (c)-(h) Comparison of the semi-analytical ring-charge mapping Eq. (9) with finite-element calculations of the Poisson-Boltzmann equation for thin and thick double layers, along various axes (insets), as well as a zoomed-in comparison (near the particle surface).

shells gives the same result as the point-charge mapping, showing that the choice of $q(\mathbf{r})$ is not unique.

Next, I generalise the point-charge mapping to mappings on line charge distributions \mathcal{C} , that are described by the parametrisation $\gamma : [a, b] \rightarrow \mathcal{C}$. While this mapping is akin to the slender-body theory for creeping flow [67], my method works also for “thick” particles, because \mathcal{C} need not coincide with the centerline of the particle. Using Eq. (3) for line charge densities $\lambda(\gamma(u))$, I find

$$\varphi(\mathbf{r}) = \ell_B \int_a^b du |\gamma'(u)| \lambda(\gamma(u)) \frac{\exp[-\kappa|\mathbf{r} - \gamma(u)|]}{|\mathbf{r} - \gamma(u)|}. \quad (7)$$

For effective pair interactions of arbitrarily positioned and oriented line charges, applying Eq. (5), I find,

$$\begin{aligned} \beta\Phi_\epsilon(\mathbf{d}, \Omega_1, \Omega_2) &= \ell_B \int_{a_1}^{b_1} du |\gamma'_1(u)| \lambda_1(\gamma_1(u)) \\ &\times \int_{a_2}^{b_2} dv |\gamma'_2(v)| \lambda_2(\gamma_2(v)) \frac{\exp[-\kappa|\gamma_1(u) - \gamma_2(v)|]}{|\gamma_1(u) - \gamma_2(v)|}. \end{aligned} \quad (8)$$

To illustrate this method, I consider the pair potential between two identical tori with inner radius R_I , outer radius R_O [Fig. 1(a)], and uniform surface charge density $\sigma = Z_t/(4\pi^2 R_I R_O)$. As a first step, I map the torus to a charged ring with parametrisation $\gamma(u) =$

$(R \cos u, R \sin u, 0)$, $u \in [0, 2\pi)$, of uniform line charge density $\lambda = Q_r/(2\pi R)$. Unlike the point-charge mapping, not only the line charge number Q_r has to be determined, but also the shape for $R \in [R_O - R_I, R_O + R_I]$. Using Eq. (7), I find,

$$\varphi(\mathbf{r}) = \frac{Z_t \ell_B \Upsilon_t}{2\pi} \int_0^{2\pi} du \frac{\exp[-\kappa\sqrt{r^2 + R^2 - 2\rho R \cos(u)}]}{\sqrt{r^2 + R^2 - 2\rho R \cos(u)}}, \quad (9)$$

with $r = \sqrt{\rho^2 + z^2}$ in cylindrical coordinates, and I factorised the ring charge $Q_r(\kappa R_O, R_I/R_O) = Z_t \Upsilon_t(\kappa R_O, R_I/R_O)$ using the linearity of Eq. (1). Note that only for $\kappa = 0$ or $\rho = 0$, the integral in Eq. (9) can be evaluated in terms of known special functions [68]. For the general case the integral can be numerically computed on a desktop PC within seconds. Secondly, to establish the values of Υ and R , I fit the surface potential $\varphi(\rho = R_O + R_I \cos \alpha, z = R_I \sin \alpha)$, with $\alpha \in [0, 2\pi)$, to the numerically obtained surface potential of a charged torus for fixed κR_O , R_I/R_O , and ϵ_p/ϵ_s [69].

For the numerically obtained axisymmetric $\phi(\mathbf{r})$ of a torus [Figs. 1(a-b)] [70], I show how the semi-analytical approximation compares for thin and thick double layers with finite-element calculations [69] for various cuts along the torus [Figs. 1(c-h)]. For weak and strong

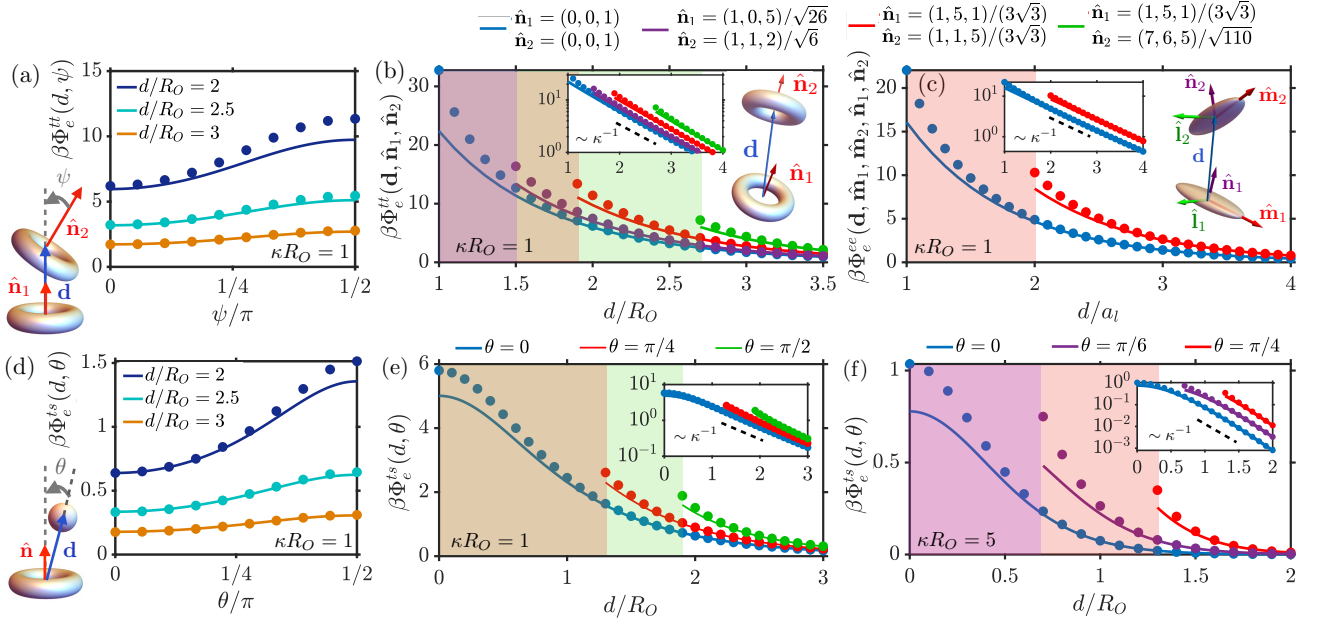


Figure 2. Semi-analytical approximation of the effective pair potential (lines) compared with finite-element calculations (dots) for various shapes, particle configurations, and screening lengths at $\ell_B/R_O = 0.01$ and $\epsilon_p/\epsilon_s = 0.2$. I consider (a-b) identical tori [Eq. (11)], (c) identical tri-axial ellipsoids [69], and (d-f) torus-sphere additive mixtures [Eq. (14)]. The coloured shaded areas indicate overlap of particle hard cores when the particle distance d is decreased at fixed orientation from $d \rightarrow \infty$. Tori have charge $Z_t = 100$ and inner radius $R_I = 0.5R_O$. Ellipsoids have the same charge, surface area, and volume as the tori with “radius” along $\hat{\mathbf{l}}_i = \hat{\mathbf{m}}_i \times \hat{\mathbf{n}}_i$ given by $a_i = R_O$. In (c) $\hat{\mathbf{m}}_1 = (-1, 1, 0)/\sqrt{2}$, $\hat{\mathbf{m}}_2 = (0, 1, 0)$ (blue) and $\hat{\mathbf{m}}_1 = (-0.722, -0.0269, 0.692)$, $\hat{\mathbf{m}}_2 = (-1, 1, 0)/\sqrt{2}$ (red). Spheres have the same surface charge density as the torus with radius $a = 0.4R_O$.

intra-particle double layer overlap, Eq. (9) agrees excellently with numerics [69], capturing the full spatial dependence of $\phi_{>}(\mathbf{r})$ for suitably chosen Υ and R , even for tori with large particle volumes. Finally, Eq. (9) gives analytical insight: for $r \rightarrow \infty$, I find that $\varphi(\mathbf{r}) \sim \mathcal{A}(\theta)Z_t\ell_B \exp(-\kappa r)/r$, with anisotropy function [69],

$$\frac{\mathcal{A}(\theta)}{\Upsilon_t} = 1 + \frac{1}{4} \sin^2 \theta (\kappa R)^2 + \frac{1}{64} \sin^4 \theta (\kappa R)^4 + \dots \quad (10)$$

showing the well-known result that particle anisotropy

still persists in the far-field electrostatic potential unlike the unscreened case, and that the anisotropies are more pronounced for large κ [36, 42]. To my best knowledge $\mathcal{A}(\theta)$ has never been calculated for a torus before.

To calculate effective pair interactions, I parametrise two identical rings with arbitrary orientations as $\gamma_i(u) = \mathbf{X}_i + R \cos u \hat{\mathbf{l}}_i + R \sin u \hat{\mathbf{m}}_i$, ($i = 1, 2$), with $\hat{\mathbf{n}}_i \cdot \hat{\mathbf{l}}_i = \hat{\mathbf{n}}_i \cdot \hat{\mathbf{m}}_i = 0$, and $\hat{\mathbf{n}}_i$ the unit normal to the plane in which the ring is situated that coincides with the plane where the outer ring of the corresponding torus is situated. Using Eq. (8), I find the interaction between two identical tori,

$$\beta \Phi_e^{tt}(\mathbf{d}, \hat{\mathbf{n}}_1, \hat{\mathbf{n}}_2) = \frac{Z_t^2 \ell_B \Upsilon_t^2}{(2\pi)^2} \int_0^{2\pi} du \int_0^{2\pi} dv \frac{\exp \left[\frac{-\kappa \sqrt{d^2 + 2R^2 - 2Rf(u, v; \mathbf{d}, \hat{\mathbf{n}}_1, \hat{\mathbf{n}}_2)}}{\sqrt{d^2 + 2R^2 - 2Rf(u, v; \mathbf{d}, \hat{\mathbf{n}}_1, \hat{\mathbf{n}}_2)}} \right]}{\sqrt{d^2 + 2R^2 - 2Rf(u, v; \mathbf{d}, \hat{\mathbf{n}}_1, \hat{\mathbf{n}}_2)}}, \quad (11)$$

for \mathbf{d} not parallel to $\hat{\mathbf{n}}_1$ and/or $\hat{\mathbf{n}}_2$, the term f in the integrand simplifies to,

$$f(u, v; \mathbf{d}, \hat{\mathbf{n}}_1, \hat{\mathbf{n}}_2) = d \sin v |\hat{\mathbf{n}}_1 \times \hat{\mathbf{n}}_2| + R [\cos(u - v) - (1 - \hat{\mathbf{n}}_1 \cdot \hat{\mathbf{n}}_2) \sin u \sin v], \quad (12)$$

whereas for \mathbf{d} not parallel to either $\hat{\mathbf{n}}_1$ or $\hat{\mathbf{n}}_2$,

$$f = |\mathbf{b}_1| \sin u - |\mathbf{b}_2| \sin v + \frac{R}{|\mathbf{b}_1||\mathbf{b}_2|} \left(\cos u \cos v [d^2(\hat{\mathbf{n}}_1 \cdot \hat{\mathbf{n}}_2) - (\mathbf{d} \cdot \hat{\mathbf{n}}_1)(\mathbf{d} \cdot \hat{\mathbf{n}}_2)] + \cos u \sin v [\mathbf{d} \cdot (\hat{\mathbf{n}}_1 \times \hat{\mathbf{n}}_2)(\mathbf{d} \cdot \hat{\mathbf{n}}_2)] - \sin u \cos v [\mathbf{d} \cdot (\hat{\mathbf{n}}_1 \times \hat{\mathbf{n}}_2)(\mathbf{d} \cdot \hat{\mathbf{n}}_1)] + \sin u \sin v \left\{ d^2(\hat{\mathbf{n}}_1 \cdot \hat{\mathbf{n}}_2)^2 - (\mathbf{d} \cdot \hat{\mathbf{n}}_1)(\mathbf{d} \cdot \hat{\mathbf{n}}_2)(\hat{\mathbf{n}}_1 \cdot \hat{\mathbf{n}}_2) + [\mathbf{d} \cdot (\hat{\mathbf{n}}_1 \times \hat{\mathbf{n}}_2)]^2 \right\} \right). \quad (13)$$

In Eq. (13), I used the parametrisation $\hat{\mathbf{l}}_i = \mathbf{b}_i/|\mathbf{b}_i|$ and $\hat{\mathbf{m}}_i = \hat{\mathbf{l}}_i \times \hat{\mathbf{n}}_i$, with vector $\mathbf{b}_i = \mathbf{d} \times \hat{\mathbf{n}}_i$ for $i = 1, 2$.

Despite being an integral representation, the evaluation of Eq. (11) is far less computationally expensive than three-dimensional finite-element calculations of Eq. (1) for every fixed particle configuration.

In Figs. 2(a-b), I compare the numerical calculation and the analytical approximation of Eqs. (11)-(13) for a wide variety of particle configurations. I find an excellent agreement, with only a deviation for particle separations close to contact where the repulsion is underestimated, as expected from a method that is equivalent to the LSA [61]. To show the generality of the framework, I also compare the interaction potentials for selected configurations of two tri-axial ellipsoids [Fig. 2(c)], for which a mapping to a spherical shell was needed, rather than a line charge [69]. I hypothesise, however, that some metal spheroidal particles can be mapped to straight lines, because the (unscreened) isopotential surfaces of straight lines are prolate spheroids with specific aspect ratios [71]. Finally, the method can also be extended to additive mixtures of particles, as I highlight for the torus-sphere interaction,

$$\beta\Phi_e^{ts}(\mathbf{d}, \hat{\mathbf{n}}) = \frac{Z_t Z_s \ell_B}{2\pi} \Upsilon_t(\kappa R_O, \kappa R_I) \Upsilon_s(\kappa a) \times \int_0^{2\pi} du \frac{\exp\left[-\kappa\sqrt{d^2 + R^2 + 2R\sin u|\mathbf{d} \times \hat{\mathbf{n}}|}\right]}{\sqrt{d^2 + R^2 + 2R\sin u|\mathbf{d} \times \hat{\mathbf{n}}|}}, \quad (14)$$

which, again, agrees excellently with numerics [Figs. 2(d-f)], even when the sphere partly enters the hole of the torus [Fig. 2(e-f), blue line]. In the insets, I highlight on log-linear scale that the decay length for these particle shapes is still κ^{-1} , however, with an orientation-dependent interaction amplitude of higher anisotropy when the salt concentration is increased [Figs. 2(e-f)], which is generic for anisotropic particles [36, 42], as is for the electrostatic potential [Eq. (10)].

Summarising, I developed a framework to derive effective pair potentials between finite-sized arbitrarily-shaped rigid macroions. With different combinations of spheres, ellipsoids, and tori in various mutual orientations I showed the applicability and accuracy of this method: this framework gives analytical insights with broad relevance for experiments and simulations. I expect that the method applies to many shapes when multiple inhomogeneous singular charge distributions are used. Furthermore, as recently shown, the method works also for spheres dispersed in nematic liquid crystals [9]. Finding the correct charge distribution for a specific particle can be non-trivial, but often symmetry arguments and an analysis of the necessary multipole moments to match the far-field electrostatic potential are useful considerations. For example, it was suggested that Janus spheres can be described by a collection of point charges [72]. My method becomes less accurate at small particle separations, like DLVO theory, where the surface potential and/or surface charge density become “polarised”, which, however, can be reconciled with the Derjaguin approxi-

mation [43, 66, 73, 74]. Furthermore, it is not possible to derive multi-body interactions (of the form as in Ref. [75]), because of the underlying LSA equivalence.

As an outlook, I propose extending the theory with (many-body) charge regulation [51, 74, 76–78] and renormalisation [79–82] to incorporate more types of electrostatic boundary conditions and non-linear screening, respectively. The expressions of this manuscript can then still be used with the bare charge replaced by an effective (renormalised) charge. More broadly, the findings might also be valuable for any physical system governed by the Helmholtz equation, e.g. acoustics [83] and optics [84], or systems where the Yukawa potential is involved, such as wetting [85]. Finally, it would be intriguing to explore charge-screened active matter for various “thick” particles. Here, the Yukawa potential is already often used to model steric repulsions between thin active rods [86, 87].

Acknowledgements I acknowledge financial support from the European Union’s Horizon 2020 programme under the Marie Skłodowska-Curie grant agreement No. 795377 and the Slovenian Research Agency ARRS under contract J1-9149. Furthermore, I benefited from fruitful discussions with M. Ravnik, M. Murko, S. Čopar, D. O’Lee, and R. Goldstein. Special thanks goes to N. Boon, who exposed me to the derivation of the DLVO potential using a point-charge mapping, which was an incentive to generalise this method to more complicated structures. M. A. Janssen, S. Čopar, and C. Schaefer are thanked for critically reading the manuscript and for providing useful comments. Finally, I would like to thank the Isaac Newton Institute for Mathematical Sciences for support and hospitality during the programme [The Mathematical Design of New Materials] when work on this paper was undertaken. This work was supported by: EPSRC grant number EP/R014604/1.

-
- [1] P. Werner and A. J. Millis, *Phys. Rev. Lett.* **104**, 146401 (2010).
 - [2] E. Mauri and H. T. C. Stoof, *J. High Energ. Phys.* **2019** (4), 35.
 - [3] J. E. Lennard-Jones and J. A. Pople, *Proc. R. Soc. Lond. A* **210**, 190 (1951).
 - [4] B. Wang and D. G. Truhlar, *J. Chem. Th. Comp.* **10**, 4480 (2014).
 - [5] K. A. Parendo, K. H. S. B. Tan, A. Bhattacharya, M. Eblen-Zayas, N. E. Staley, and A. M. Goldman, *Phys. Rev. Lett.* **94**, 197004 (2005).
 - [6] G. Schreiber and A. R. Fersht, *Nat. Struct. Mol. Biol* **3**, 427 (1996).
 - [7] K. Kočevar and I. Muševič, *Phys. Rev. E* **65**, 030703 (2002).
 - [8] H. Mundoor, B. Senyuk, and I. I. Smalyukh, *Science* **352**, 69 (2016).
 - [9] J. C. Everts, B. Senyuk, H. Mundoor, M. Ravnik, and I. I. Smalyukh, Anisotropic electrostatic and elas-

- tic interactions of charged colloidal spheres (2020), [arXiv:2005.05682](https://arxiv.org/abs/2005.05682) [cond-mat.soft].
- [10] H. H. Strey, V. A. Parsegian, and R. Podgornik, *Phys. Rev. Lett.* **78**, 895 (1997).
- [11] A. A. Kornyshev, D. J. Lee, S. Leikin, and A. Wynveen, *Rev. Mod. Phys.* **79**, 943 (2007).
- [12] D. J. Lee, *J. Phys.: Condens. Matter* **23**, 105102 (2011).
- [13] E. H. Hwang and S. Das Sarma, *Phys. Rev. B* **75**, 205418 (2007).
- [14] R. E. Goldstein, A. I. Pesci, and V. Romero-Rochn, *Phys. Rev. A* **41**, 5504 (1990).
- [15] D. Andelman, in *Handbook of biological physics*, Vol. 1 (Elsevier, 1995) pp. 603–642.
- [16] J. R. Miller and P. Simon, *Science* **321**, 651 (2008).
- [17] S. Kondrat and A. Kornyshev, *J. Phys.: Condens. Matter* **23**, 022201 (2010).
- [18] M. Z. Bazant and T. M. Squires, *Phys. Rev. Lett.* **92**, 066101 (2004).
- [19] H. Thomas, G. E. Morfill, V. Demmel, J. Goree, B. Feuerbacher, and D. Möhlmann, *Phys. Rev. Lett.* **73**, 652 (1994).
- [20] P. Hopkins, A. J. Archer, and R. Evans, *Phys. Rev. E* **71**, 027401 (2005).
- [21] S. C. Glotzer and M. J. Solomon, *Nat. Mater* **6**, 557 (2007).
- [22] M. A. Boles, M. Engel, and D. V. Talapin, *Chem. Rev* **116**, 11220 (2016).
- [23] N. D. Lang and W. Kohn, *Phys. Rev. B* **1**, 4555 (1970).
- [24] T. L. Einstein and J. R. Schrieffer, *Phys. Rev. B* **7**, 3629 (1973).
- [25] J. Friedel, *Il Nuovo Cimento* (1955-1965) **7**, 287 (1958).
- [26] P. Debye and E. Hückel, *Phys. Z* **24**, 185 (1923).
- [27] L. H. Thomas, *Math. Proc. Camb. Philos. Soc* **23**, 542–548 (1927).
- [28] E. Fermi, *Z. Phys.* **48**, 73 (1928).
- [29] A. Yethiraj and A. van Blaaderen, *Nature* **421**, 513 (2003).
- [30] B. Derjaguin and L. Landau, *Acta Physicochim. URSS* **14**, 633 (1941).
- [31] E. J. W. Verwey and J. T. G. Overbeek, in *Theory of the Stability of Lyophobic Colloids* (Elsevier, New York, 1948).
- [32] I will only consider the electrostatic part of the full DLVO potential in this letter.
- [33] L. Belloni, *J. Phys. Condens. Matter* **12**, R549 (2000).
- [34] A. Zacccone, H. Wu, D. Gentili, and M. Morbidelli, *Phys. Rev. E* **80**, 051404 (2009).
- [35] D. G. Rowan, J.-P. Hansen, and E. Trizac, *Mol. Phys.* **98**, 1369 (2000).
- [36] E. Trizac, L. Bocquet, R. Agra, J.-J. Weis, and M. Aubouy, *J. Phys.: Cond. Matt.* **14**, 9339 (2002).
- [37] R. Agra, E. Trizac, and L. Bocquet, *Eur. Phys. J E* **15**, 345–357 (2004).
- [38] S. Jabbari-Farouji, J.-J. Weis, P. Davidson, P. Levitz, and E. Trizac, *J. Chem. Phys.* **141**, 224510 (2014).
- [39] S. L. Brenner and V. Parsegian, *Biophys. J.* **14**, 327 (1974).
- [40] E. Eggen, M. Dijkstra, and R. van Roij, *Phys. Rev. E* **79**, 041401 (2009).
- [41] J.-P. Hsu and B.-T. Liu, *J. Colloid Interface Sci* **190**, 371 (1997).
- [42] C. Álvarez and G. Téllez, *J. Chem. Phys.* **133**, 144908 (2010).
- [43] P. Schiller, S. Krüger, M. Wahab, and H.-J. Mögel, *Langmuir* **27**, 10429 (2011).
- [44] M. Heinen, F. Zanini, F. Roosen-Runge, D. Fedunová, F. Zhang, M. Hennig, T. Seydel, R. Schweins, M. Sztucki, M. Antalík, F. Schreiber, and G. Nägele, *Soft Matter* **8**, 1404 (2012).
- [45] V. Jadhao, Z. Yao, C. K. Thomas, and M. O. de la Cruz, *Phys. Rev. E* **91**, 032305 (2015).
- [46] A. A. Kornyshev and S. Leikin, *J. Chem. Phys.* **107**, 3656 (1997).
- [47] J.-P. Hsu and B.-T. Liu, *J. Phys. Chem. B* **102**, 3892 (1998).
- [48] M. Fushiki, *J. Chem. Phys.* **97**, 6700 (1992).
- [49] H. Löwen, P. A. Madden, and J.-P. Hansen, *Phys. Rev. Lett.* **68**, 1081 (1992).
- [50] Y. Hallez, J. Diatta, and M. Meireles, *Langmuir* **30**, 6721 (2014).
- [51] J. C. Everts, N. Boon, and R. van Roij, *Phys. Chem. Chem. Phys.* **18**, 5211 (2016).
- [52] A.-P. Hynninen and M. Dijkstra, *Phys. Rev. E* **68**, 021407 (2003).
- [53] S. Jabbari-Farouji, H. Tanaka, G. H. Wegdam, and D. Bonn, *Phys. Rev. E* **78**, 061405 (2008).
- [54] M. E. Leunissen, C. G. Christova, A.-P. Hynninen, C. P. Royall, A. I. Campbell, A. Imhof, M. Dijkstra, R. van Roij, and A. van Blaaderen, *Nature* **437**, 235 (2005).
- [55] K. Miszta, J. De Graaf, G. Bertoni, D. Dorfs, R. Brescia, S. Marras, L. Ceseracciu, R. Cingolani, R. van Roij, M. Dijkstra, *et al.*, *Nat. Mater* **10**, 872 (2011).
- [56] A. P. Gantapara, J. de Graaf, R. van Roij, and M. Dijkstra, *Phys. Rev. Lett.* **111**, 015501 (2013).
- [57] A. Haji-Akbari, M. Engel, and S. C. Glotzer, *J. Chem. Phys.* **135**, 194101 (2011).
- [58] P. F. Damasceno, M. Engel, and S. C. Glotzer, *Science* **337**, 453 (2012).
- [59] B. De Nijs, S. Dussi, F. Smalenburg, J. D. Meeldijk, D. J. Groenendijk, L. Filion, A. Imhof, A. Van Blaaderen, and M. Dijkstra, *Nat. Mater* **14**, 56 (2015).
- [60] S. Dussi and M. Dijkstra, *Nat. Commun* **7**, 11175 (2016).
- [61] S. L. Carnie and D. Y. Chan, *J. Coll. Int. Sci.* **155**, 297 (1993).
- [62] B. Duplantier, R. E. Goldstein, V. Romero-Rochn, and A. I. Pesci, *Phys. Rev. Lett.* **65**, 508 (1990).
- [63] V. Weston, *Quart. Appl. Math.* **16**, 237 (1958); *J. Math. Phys.* **39**, 64 (1960).
- [64] A. Enriquez and L. Blum, *Mol. Phys* **103**, 3201 (2005).
- [65] V. A. Andreev and A. I. Victorov, *Langmuir* **22**, 8298 (2006); *Mol. Phys* **105**, 239 (2007).
- [66] G. Bell, S. Levine, and L. McCartney, *J. Colloid Interface Sci.* **33**, 335 (1970).
- [67] J. B. Keller and S. I. Rubinow, *J. Fluid Mech* **75**, 705–714 (1976).
- [68] O. Ciftja, A. Babineaux, and N. Hafeez, *Eur. J. Phys.* **30**, 623 (2009).
- [69] See the Supplemental information for: (i) details of the numerical finite-element calculations, (ii) determination of the charge parameters and shape parameters of charged tori and tri-axial ellipsoids, (iii) expressions for the electrostatic potential and the effective pair interaction for tri-axial ellipsoids, (iv) comparisons of the electrostatic potential and pair interactions for tori at more values of κR_O and R_I/R_O , (v) derivation of the anisotropy function of a single torus from a Yukawa multipole expansion.

- [70] J. C. Everts and M. Ravnik, *Sci. Rep.* **8**, 14119 (2018).
- [71] T. L. Curtright, N. M. Aden, X. Chen, M. J. Haddad, S. Karayev, D. B. Khadka, and J. Li, *Eur. J. Phys.* **37**, 035201 (2016).
- [72] J. de Graaf, N. Boon, M. Dijkstra, and R. van Roij, *J. Chem. Phys.* **137**, 104910 (2012).
- [73] S. Dorosz, N. Shegokar, T. Schilling, and M. Oettel, *Soft Matter* **10**, 4717 (2014).
- [74] A. P. dos Santos and Y. Levin, *Phys. Rev. Lett.* **122**, 248005 (2019).
- [75] M. Brunner, J. Dobnikar, H.-H. von Grünberg, and C. Bechinger, *Phys. Rev. Lett.* **92**, 078301 (2004).
- [76] H. H. von Grünberg, *J. Coll. Int. Sci.* **219**, 339 (1999).
- [77] J. C. Everts, M. N. van der Linden, A. van Blaaderen, and R. van Roij, *Soft Matter* **12**, 6610 (2016).
- [78] T. Markovich, D. Andelman, and R. Podgornik, *EPL* **113**, 26004 (2016).
- [79] S. Alexander, P. M. Chaikin, P. Grant, G. J. Morales, P. Pincus, and D. Hone, *J. Chem. Phys.* **80**, 5776 (1984).
- [80] E. Trizac and Y. Levin, *Phys. Rev. E* **69**, 031403 (2004); S. Pianegonda, E. Trizac, and Y. Levin, *J. Chem. Phys.* **126**, 014702 (2007).
- [81] Y. Jho, J. Landy, and P. A. Pincus, *ACS Macro Lett.* **4**, 640 (2015).
- [82] N. Boon, G. I. Guerrero-García, R. van Roij, and M. Olvera de la Cruz, *Proc. Natl. Acad. Sci. U.S.A* **112**, 9242 (2015).
- [83] T. Miloh, *Acoust. Phys.* **62**, 663–671 (2016).
- [84] R. P. Feynman, R. B. Leighton, and M. Sands, *The Feynman lectures on physics, Vol. I: The new millennium edition: mainly mechanics, radiation, and heat*, Vol. 1 (Basic books, 2011).
- [85] M. T. da Gama and R. Evans, *Mol. Phys* **48**, 687 (1983).
- [86] D. Winter, J. Horbach, P. Virnau, and K. Binder, *Phys. Rev. Lett.* **108**, 028303 (2012).
- [87] A. Kaiser, H. H. Wensink, and H. Löwen, *Phys. Rev. Lett.* **108**, 268307 (2012).